Complex-valued independent component analysis of natural images

Valero Laparra [†], Michael U. Gutmann[*], Jesús Malo [†], and Aapo Hyvärinen [*]

[†] Image Processing Laboratory (IPL),
Universitat de València, Spain

[*] Department of Computer Science
Department of Mathematics and Statistics
Helsinki Institute for Information Technology HIIT
P.O. Box 68, FIN-00014 University of Helsinki, Finland

Abstract. Linear independent component analysis (ICA) learns simple cell receptive fields from natural images. Here, we show that linear complex-valued ICA learns complex cell properties from Fourier-transformed natural images, i.e. two Gabor-like filters with quadrature-phase relationship. Conventional methods for complex-valued ICA assume that the phases of the output signals have uniform distribution. We relax this assumption by modeling of the phase information of the output sources in the complex-valued ICA estimation. The resulting model of phases shows that the distributions are often far from uniform, and the shapes of the Gabor filters are also changed.

Keywords: Complex Independent Components Analysis, Natural Image Statistics, Modeling Fourier phase distribution

1 Introduction

Natural image statistics has become a very useful tool in order to understand how the visual part of the brain works (see for instance [1] for review). One of the most relevant revelations has been that a set of linear sensors optimized to obtain independent sources from natural image data resembles the Gabor-like receptive fields in the primary visual cortex (V1) [2, 3].

In recent years, the advances in natural image statistics have been mainly in describing the statistics of the signals after this linear "simple cell" stage [4–9]. A common point of these models is that they focus on the total magnitude of the sensor (simple cell) outputs. Often, a combination of the squared outputs of simple cells is learned, leading to something like complex cells. However, there is evidence that relative magnitude, or phase, of simple cells plays an important role. A simple example about the relative importance of the magnitude and phase can be found in [10]. In this example the magnitude and the phase in the Fourier domain of two images were exchanged, and the images which were perceptually more similar to the originals were the ones that carried the phase information. Moreover there is experimental evidence of phase coupled Gabor-like filters in V1 [12, 11]. For this reason, Daugman [13] suggested that the receptive field in

the first stage could be seen as Gabor sensors defined in the complex domain: the real and the imaginary part are essentially the same Gabor filter but with phases in quadrature.

Despite the evidences of the importance of the phase, not too much progress has been made in statistically modeling the phase of the signals after the simple cell step. The contributions in this field are restricted to models with a fixed linear stage, the wavelet transform [14, 15]. Although this led to interesting results about the distribution of natural images, the statistics used in this kind of modeling could depend on the particular choice of using the wavelet transform as first linear stage.

Here, we aim at both modeling the phase distribution and learning the first linear stage from the data. For that purpose, we are proposing a extension of complex independent component analysis (cICA) [16]. The proposed extension deals with explicit modeling the phase of non-circularly symmetric sources as an alternative to [17], which does consider non-symmetric sources but it does not model the lack of symmetry.

The paper falls naturally in two parts. In Section 2, we review cICA and point out its limitations in modeling the phase distribution. Section 3 shows how cICA can be extended to better capture the distribution of the phase variable. The extension includes the version of [16] as special case. Although we focus here on natural images, the extension can be applied to all kinds of data. Conclusions are drawn in Section 4.

2 Complex Independent Component Analysis and its limitations

2.1 Complex Independent Component Analysis

As in Independent Component Analysis (ICA) for real variables, the goal in complex ICA (cICA) [16] is to find a linear transformation W such that, when applied to some vector of signals x, the elements of the output vector $s = W^H x$ are statistically as independent as possible. The difference to real ICA is that W, x, and hence also s are complex valued. Furthermore, instead of the transpose W^T, the transposed, complex conjugate W^H is used.

In ICA, one approach to find such a W is to first whiten the data and then to maximize the kurtosis, or a statistically more robust contrast function. In cICA, the same approach can be taken by appropriately defining whitening and choosing an appropriate contrast function.

For complex variables, the random vector x is white if both the real and imaginary part can be defined to be white and if the real and imaginary parts are uncorrelated. An equivalent condition is that $\mathbb{E}\{xx^H\} = I$ and $\mathbb{E}\{xx^T\} = 0$. Denoting a column of W by w_i, in [16], cICA can be performed by optimization of J_G,

$$J_G(W) = \sum_{i=1}^{n} \mathbb{E}\{G(|w_i^H x|^2)\}, \tag{1}$$

under the constraint $W^H W = I$. Depending on the nature of the sources, J_G needs to be maximized or minimized. The contrast function G must be a smooth even function and x is assumed to be white. Possible candidates include $G(y) = -\sqrt{a + y^2}$ for a small constant a. In the simulations in the next section, we will use this contrast function with $a = 0.1$. Note that the objective function depends only on the moduli $r_i = |w_i^H x|$ of the complex variable $s_i = w_i^H x$, no matter the choice of G. For sparse sources, maximization of this G leads to consistent estimators [16].

An alternative viewpoint of cICA is based on maximum likelihood estimation of the statistical model $x = Ws$ where x and s are white and $W^H W = I$. Assuming independence of the sources in $s = (s_1, \ldots, s_n)$, the log-likelihood is

$$\ell(W) = \sum_t \sum_{i=1}^{n} \log p_{s_i}(w_i^T x_t), \tag{2}$$

where x_t is the t-th observation of x and p_{s_i} is the density of the sources s_i. Since the variables are complex valued, $p_{s_i}(s_i)$ is a bidimensional distribution that can be written as $p_{r\phi}(r_i, \phi_i)/r_i$, where r_i is the modulus and ϕ_i is the phase of s_i. Assuming further that the modulus and the phase are independent and that, importantly for the next sections, the distribution of the phase is a uniform distribution, maximization of ℓ becomes maximization of

$$J_2(W) = \sum_t \sum_{i=1}^{n} \left(\log p_r(r_{it}) - \log r_{it}\right). \tag{3}$$

The term p_r denotes the distribution for the moduli r_i, where we assume that all of them follow the same distribution. Replacing sample average by expectation, we obtain the objective function in Eq.1 with $G(r^2) = \log p_r(r) - \log r$. Note further that the distribution p_q of the squared modulus $q = r^2$ is $p_q(q) = p_r(r)/(2r)$. This means that $G(q) = \log p_q(q) + \log 2$. Hence, the contrast function G used in cICA can be directly related to the distribution of the squared moduli of the complex sources. In particular, we can relate the contrast function $G(q) = -\sqrt{a + q^2}$, where a is a small constant, to the choice of p_q being a Gamma distribution,

$$p_q(q) = q^{k-1} \frac{\exp \frac{-q}{\theta}}{\Gamma(k)\theta^k}, \tag{4}$$

with $k = 1$. Then, $\log p_q(q) = -q + \text{const}$, which is, up to additive constants, the same as the above contrast function when a is small.

2.2 Simulations with natural Images

We apply cICA on natural images in the Fourier domain. The natural images are 16×16 patches extracted from the data base in [18]. The data x on which we apply cICA are the complex Fourier coefficients. For the visualization, we show the learned W combined with the whitening matrix and the Fourier transform.

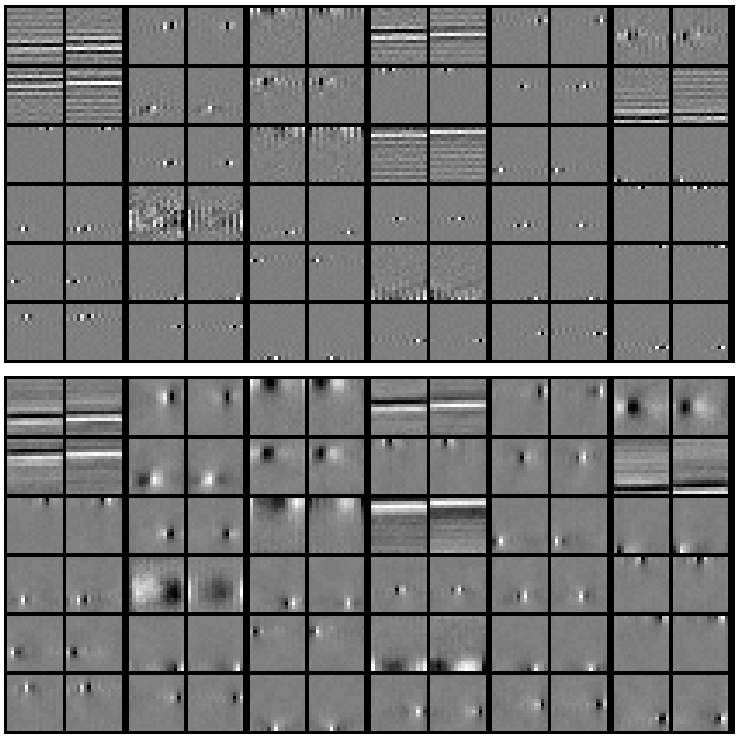

Fig. 1. Filters and features (defined by the pseudoinverse of the filter matrix) obtained with cICA using the algorithm in [16], ordered according to contrast function value (first 36 of 126). Filters and features are shown in pairs, with the real part at the left and the imaginary part at the right. Top: complex filters. Bottom: complex features.

Figure 1 shows the results. The real and the imaginary part of the complex filters obtained are shown in pairs from left to the right. Real and imaginary parts in Figure 1 display a quadrature-phase relationship. This statistical result is consistent with measurements in V1 [12, 11] and related empirical models [13]. Complex ICA results essentially replicate those obtained by independent subspace analysis [4], but the complex-valued formalism automatically creates two-dimensional subspaces in ordinary linear ICA.

2.3 Checking model assumptions

Here we check whether, for natural images, the obtained complex sources s_i follow the assumption in cICA that the (squared) moduli follow a Gamma distribution and the phases are uniformly distributed.

Fitting gamma distributions to the empirical distributions of the modulus of the sources leads to good fits, see Figure 2. In contrast, the empirical distributions of the phases do not follow the model assumptions, as shown in Figure 3. The clearly visible oscillations in the phases violate the assumption of uniformity in

cICA. These roughly bimodal histograms may be modeled by a modified Von Mises distribution to account for the two peaks,

$$p_\phi(\phi|k,\mu) = \frac{1}{2\pi I_0(k)} e^{k\cos(2(\phi-\mu))}, \tag{5}$$

where $I_0(k)$ is the Bessel function of order 0. In contrast to the ordinary von Mises distribution, we have here introduced the factor 2 inside the cosine to model the two-peaked distributions seen in fig. 3. Note that this distribution correspond to a uniform distribution when the parameter $k = 0$. In figure 3 we can see how fitting this distribution to the empirical distribution of the phase is much more precise than fitting a uniform distribution.

3 Extension of complex ICA

In this section we propose an extension of cICA. The extension builds on the maximum likelihood approach to cICA in Eq. 2. It will take into account that the distribution of the phase variables can be non-uniform, as found in natural images (Eq. 5 and Fig. 3).

As in the previous section, we write in Eq. 2 p_{s_i} as $p_{r\phi}(r_i, \phi_i)/r_i$, where r_i is the modulus and ϕ_i is the phase of s_i. Also as previously, we assume that

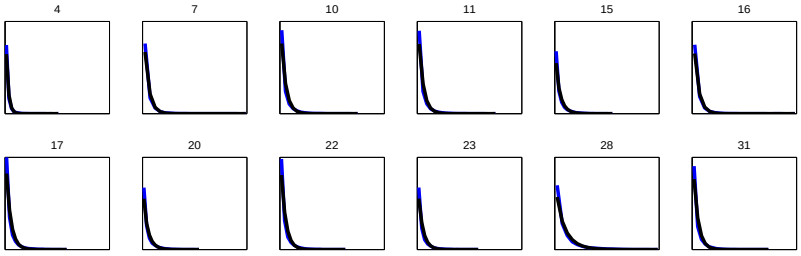

Fig. 2. Selection of distributions of the modulus of the cICA sources (blue) and a fitted gamma distribution (black). The curves are strongly overlapping and thus not clearly visible. Numbers refer to the corresponding sensor in the figure 1 (left to right, top to bottom).

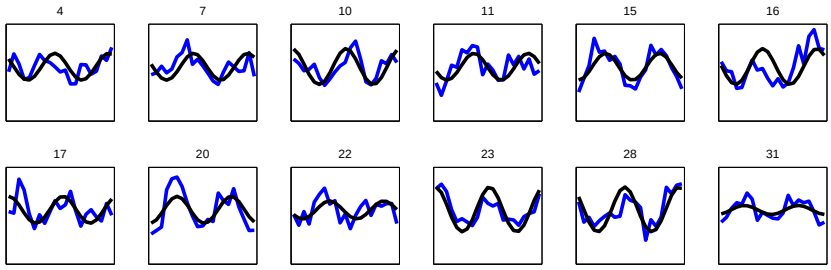

Fig. 3. Selection of distributions of the phases of the cICA sources (blue) and a fitted modified Von Mises distribution (black). Numbers refer to the corresponding sensor in the figure 1 (left to right, top to bottom).

the modulus and the phase are independent. However, instead of assuming a uniform distribution for the phases, we assume the distribution in Eq. 5. Since this distribution includes the uniform distribution, our extension includes the conventional cICA as a special case. With these assumptions, the maximum likelihood principle leads us to maximize the following objective function

$$J_{GQ}(W) = \sum_i \mathbb{E}\{G(r_i) + Q(\phi_i, k_i)\}. \tag{6}$$

Here, r_i is the modulus of the complex number $w_i^H x$, and ϕ_i is its phase. As before, w_i denotes a column of the matrix W and we have the constraint $W^H W = I$. The function G is, as before, related to the distribution of the squared modulus. A possible choice is $G(y) = -\sqrt{a + y^2}$. The function Q is related to the distribution of the phase and is given by $Q(\phi_i) = k_i \cos(2\phi_i)$, and depends on the w_i and the shape parameters k_i. Here, we can set $\mu = 0$ because this phase localization parameter is redundant: the phase of the oscillations will be determined by the estimated features anyway.

This modification of cICA can also be considered from an information theoretical point of view. The main goal of all ICA-based algorithms is to obtain independent sources, which is equivalent to reduce the mutual information (MI) between them. Therefore, as $MI(s_1, s_2, ..., s_n) = \sum_i \{h(r_i) + h(\phi_i)\} - h(s_1, s_2, ..., s_n)$, where $h(\cdot)$ is the entropy. This result can be derived by using the same assumptions as in section 2.1. Accordingly, we have to reduce the entropy of r_i and ϕ_i, (the joint entropy is invariant under unitary transforms). Note that the uniform distribution is the one with maximum entropy when the domain is bounded. Therefore, anything different to a uniform phase distribution will have less entropy, which means less MI between the variables, and hence more independent sources.

Figure 4 shows the results when the above extended cICA is applied to natural images (same setup as before). Note how the shape of the filters is more elongated (especially the highest-ranked ones) and spatially more extended than for the classical cICA. In figure 5 we can see the distribution of phases of the sources obtained with the proposed algorithm. The distributions are similar to the proposed modified Von Mises distribution.

4 Conclusions

In this paper, we have started with modeling natural images with complex Independent Component Analysis (cICA). This led to the emergence of complex filter where the real and the imaginary part have the same Gabor-like shape (same orientation and same frequency) but a difference in the phases of $\frac{\pi}{2}$.

Checking the model assumptions in cICA, we have noticed that the assumption of uniformity of the phases is often violated for natural image data. This led us to formulate an extension of cICA which models also the phase distributions. Simulations with natural images showed that the empirical distribution of the phases provide a good match to the assumptions of the extended model.

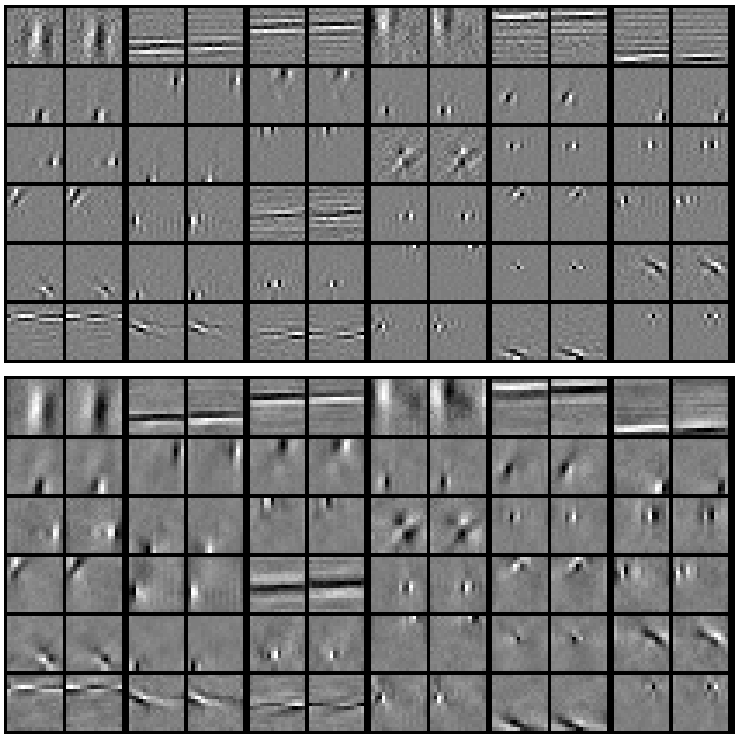

Fig. 4. Filters and features obtained with the extended cICA, ordered according to contrast function value (first 36 of 126). Filters and features are shown in pairs with the real part at the left and the imaginary part at the right. Top: complex filters. Bottom: complex features.

Our research has the potential for more extensions. For instance, the assumption of the independence between modulus and phase should be investigated more carefully.

References

1. E. P. Simoncelli and B. A. Olshausen, "Natural image statistics and neural representation.," *Annual Review of Neuroscience*, vol. 24, no. 1, pp. 1193–1216, 2001.
2. B. Olshausen and D. Field, "Emergence of simple-cell receptive field properties by learning a sparse code for natural images," *Nature*, 381: 607-609, 1996.
3. A. J. Bell and T. J. Sejnowski, "The 'Independent Components' of Natural Scenes are Edge Filters," *Vision Research*, vol. 37, no. 23, pp. 3327–3338, 1997.
4. A. Hyvärinen and P. Hoyer, "Emergence of phase- and shift-invariant features by decomposition of natural images into independent feature subspaces.," *Neural computation*, vol. 12, no. 7, pp. 1705–1720, 2000.
5. J. Portilla, V. Strela, M. Wainwright, and E. Simoncelli, "Image denoising using scale mixtures of Gaussians in the wavelet domain," 2003.

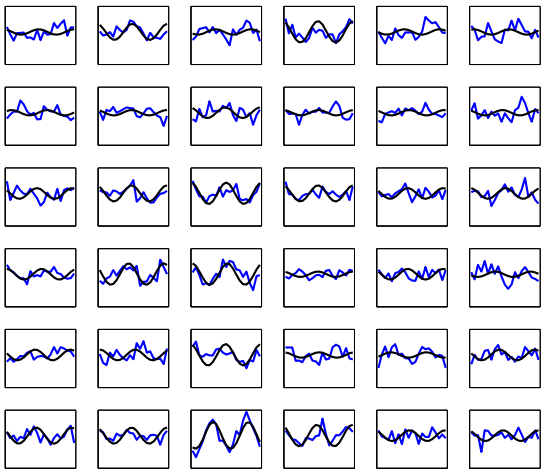

Fig. 5. Phase distributions of the sources obtained using the modified cICA algorithm corresponding to the filters and features of the figure 4. Empirical distributions in blue and fitted modified Von Mises distribution in black

6. A. Hyvärinen and U. Köster, "Complex cell pooling and the statistics of natural images.," *Network*, pp. 1–20, 2007.
7. S. Lyu and E. P. Simoncelli, "Nonlinear extraction of independent components of natural images using radial gaussianization.," *Neural computation*, vol. 21, no. 6, pp. 1485–1519, 2009.
8. J. Eichhorn, F. Sinz, and M. Bethge, "Natural image coding in V1: how much use is orientation selectivity?," *PLoS computational biology*, vol. 5, no. 4, 2009.
9. J. Malo and V. Laparra, "Psychophysically Tuned Divisive Normalization factorizes the PDF of Natural Images," *Neural computation*, vol. 22, no. 12, 2010.
10. A. V. Oppenheim and J. S. Lim, "The importance of phase in signals," *Proceedings of the IEEE*, vol. 69, no. 5, pp. 529–541, 1981.
11. J. Touryan, G. Felsen, and Y. Dan, "Spatial structure of complex cell receptive fields measured with natural images.," *Neuron*, vol. 45, no. 5, pp. 781–791, 2005.
12. D. A. Pollen and S. F. Ronner, "Phase relationships between adjacent simple cells in the visual cortex," *Science*, vol. 212, no. 4501, pp. 1409–1411, 1981.
13. J. G. Daugman, "Quadrature-phase simple-cell pairs are appropriately described in complex analytic form," *J. Opt. Soc. Am. A*, vol. 10, no. 2, pp. 375–377, 1993.
14. J. Portilla and E. P. Simoncelli, "A Parametric Texture Model Based on Joint Statistics of Complex Wavelet Coefficients," *International Journal of Computer Vision*, vol. 40, no. 1, pp. 49–70, 2000.
15. C Cadieu, *Probabilistic Models of Phase Variables for Visual Representation and Neural Dynamics*, Ph.D. thesis, UC Berkeley, 2009.
16. E. Bingham and A. Hyvärinen, "A fast fixed-point algorithm for independent component analysis of complex valued signals," *International Journal of Neural Systems*, vol. 10, pp. 1–8, 2000.
17. J. Eriksson and A.M. Seppola and V. Koivunen, "Complex ICA for circular and non-circular sources," *Proc. EUSIPOCO*, 2005.
18. A. Olmos and F.A Kingdom, "Mcgill calibrated color image database," 2004.